Journal of Power Sources 192 (2009) 285–290

Contents lists available at ScienceDirect

Journal of Power Sources

journal homepage: www.elsevier.com/locate/jpowsour

A facile method to synthesize well-dispersed $PtRuMoO_x$ and $PtRuWO_x$ nanoparticles and their electrocatalytic activities for methanol oxidation

Tao Huang, Deng Zhang, Leigang Xue, Wen-Bin Cai, Aishui Yu*

Department of Chemistry, Shanghai Key Laboratory of Molecular Catalysis and Innovative Materials, Institute of New Energy, Fudan University, 220 Handan Road, Shanghai 200433, China

ARTICLE INFO

Article history:
Received 9 February 2009
Received in revised form 18 March 2009
Accepted 18 March 2009
Available online 27 March 2009

Keywords:
DMFC
Methanol oxidation
$PtRuMoO_x$
$PtRuWO_x$

ABSTRACT

$PtRuMoO_x$ and $PtRuWO_x$ catalysts supported on multi-wall carbon nanotubes (MWCNTs) are prepared by ultrasonic-assisted chemical reduction method. XRD measurements indicate that Pt exists as face-centered cubic structure, Ru is alloyed with platinum, and the metal oxides exist as an amorphous structure. TEM pictures show that $PtRuMoO_x$ and $PtRuWO_x$ catalysts are well dispersed on the surface of MWCNTs with the particle size of about 3 nm and a narrow particle size distribution. The electrochemical properties of the catalysts for methanol electrooxidation are studied by cyclic voltammetry (CV), chronoamperometry (CA) and chronopotentiometry (CP). The onset potentials for methanol oxidation on $PtRuMoO_x$ and $PtRuWO_x$ are more negative than that of pure Pt catalyst, shifting negatively by about 0.20 V and have better electrocatalytic activities than PtRu/MWCNTs.

1. Introduction

In recent years, a lot of works have been devoted to developing suitable catalysts for methanol electrooxidation due to their potential application in direct methanol fuel cells (DMFCs) [1–3]. As the main active ingredient for methanol electrooxidation, Pt can be easily poisoned by reaction intermediates such as CO_{ads} [4–6]. In order to reduce the poisoning effect and thus improve the catalyst performance, platinum alloys have been extensively investigated [7]. For example, platinized lead deposits Pt(Pb) were prepared by a two-step electrodeposition–electroless deposition process [8]. Intermetallic compounds PtPb and PtBi for methanol oxidation were synthesized by borohydride reduction [9]. Lots of binary catalysts have been reported and PtRu is considered as the best binary alloyed catalyst because Ru takes part in a bifunctional mechanism with part of Ru atoms in oxidized state supplying oxygenated species necessary for complete oxidation of methanol to CO_2 and other part of Ru atoms alloyed with Pt weakening Pt–CO bond [10]. However, because of the still insufficient efficiency and high cost of PtRu, further optimization of the catalyst is crucial and significant for its practical application. The most common solution is to employ tri-metallic catalysts with other cheap metals or metal oxides, and disperse the catalysts on proper supports. Ternary metal catalysts PtRuSn [11,12] and PtRuM (M = Au, Co, Cu, Fe, Ni, W, Sn, Mo) synthesized via impregnation [13], colloid methods [14] and electrochemical deposition [15] have been reported for methanol electrooxidation. $PtRuMO_x$ (M = W, Mo, V) catalysts by adding non-noble metal oxides to PtRu [16–18] also showed improved electro-catalytic performance as the mixed oxides are capable of adsorbing large quantities of OH species and have multiple valences that could reduce Pt poisoning and promote methanol oxidation [19,20].

It is well known that the electrocatalytic activity of a catalyst for methanol oxidation depends strongly on its particle size, morphology and particle distribution. Highly dispersed catalyst with a small particle size and a narrow size distribution are desirable due to its large surface-to-volume ratio and facile access to each catalyst particle [21]. Proper support such as carbon nanotubes (CNTs) [22,23] with high mechanical resilience, high electrical conductivity and large surface area could be an ideal support for catalysts to generate higher electrochemical reactive surface area, however, preparation of well-dispersed catalysts on CNTs remains a challenge. In this study, a facile method, i.e. an ultrasonic-assisted chemical reduction, to prepare well-dispersed $PtRuMoO_x$ and $PtRuWO_x$ catalysts supported on MWCNTs was proposed and the effect of non-noble metal oxide MoO_x and WO_x on PtRu catalyst performance for methanol electrooxidation was investigated.

2. Experimental

2.1. Preparation of catalysts

Multi-wall carbon nanotubes with a diameter range of 20–30 nm and 30 μm length were used as the supports. K_2PtCl_6, $RuCl_3$,

* Corresponding author. Tel.: +86 21 55664259; fax: +86 21 65642403.
E-mail address: asyu@fudan.edu.cn (A. Yu).

0378-7753/$ – see front matter © 2009 Elsevier B.V. All rights reserved.
doi:10.1016/j.jpowsour.2009.03.037

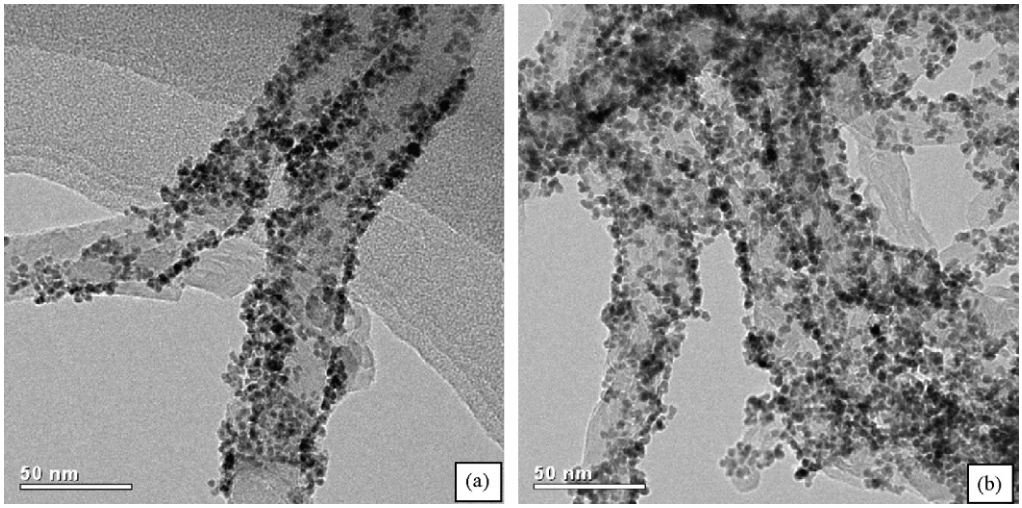

Fig. 1. TEM images of (a) $PtRuMoO_x$/MWCNTs; (b) $PtRuWO_x$/MWCNTs.

$Na_2MoO_4{\cdot}2H_2O$, $Na_2WO_4{\cdot}2H_2O$ and other chemicals were all of analytical grade and used without further purification.

For MWCNTs-supported $PtRuMoO_x$ and $PtRuWO_x$ catalyst synthesis, MWCNTs were firstly ultrasonicated in a solution containing isopropanol and H_2O (with a volume ratio of 1:1) for 20 min, and then a certain amount of the corresponding metallic salts of K_2PtCl_6, $RuCl_3$, $Na_2MoO_4{\cdot}2H_2O$, $Na_2WO_4{\cdot}2H_2O$ were added to the above solution with Pt:Ru:Mo (or W) molar ratio of 6:3:1. The content of MWCNTs was fixed at 75 wt%. After that, a solution of 0.04 M KBH_4 and 0.005 M KOH was added dropwise and the resulting suspension was maintained under ultrasonication at 50–55 °C for 2 h to allow a complete reduction of metallic salt. Filtration the solution and the solid product was collected, washed thoroughly with water and ethanol, and finally dried at 80 °C overnight. Pt, PtRu (the molar ratio of Pt to Ru is 2:1) supported on MWCNTs with a same catalyst load were also prepared by similar procedures for comparison.

2.2. Catalyst characterization

The as-prepared catalysts were characterized by powder X-ray diffraction (XRD), which was carried out on a Bruker D8 Advance X-ray diffractometer using Cu Kα radiation with a λ of 1.5406 Å at a scan rate of 4 deg min^{-1}. The morphology of catalysts was observed by transmission electron microscopy (TEM, JEOL JEM-2010) with an accelerating voltage of 200 kV. The composition was analyzed by energy-dispersive X-ray (EDX) spectrometry (Oxford, INCA, attached to TEM).

2.3. Preparation of working electrodes

The working electrode for electrochemical measurement was prepared by thin film electrode method. The glassy carbon electrode (GC, Ø5 mm) sealed by PTFE was used as substrate, which was polished with 0.05 μm alumina powder, until a shiny, mirror-like surface was obtained, and was ultrasonicated for several minutes in deionized water. 5 mg of the as-prepared catalysts were dispersed in 1.8 ml isopropanol solution, and ultrasonicated for 20 min subsequently. 10 μl suspensions were carefully transferred onto a GC substrate. After solvent evaporation, the deposited catalysts (28 $\mu g_{metal}\,cm^{-2}$) was covered with 3 μl Nafion solution (0.5 wt%, Dupont) in order to fix the particles on the substrate. The resulting Nafion film with a thickness of ≤0.2 μm had a sufficient strength to attach the catalysts to the GC substrate without producing film diffusion resistances [24].

2.4. Electrochemical characterization and measurements

Before electrochemical measurement for methanol oxidation, the working electrodes were characterized in 0.5 M H_2SO_4 solution at a scan rate of 50 mV s^{-1} by CV. The catalytic activities of the as-prepared catalysts for methanol oxidation were studied by means of CV and CA. The CV measurements were carried out in a solution of 0.5 M CH_3OH and 0.5 M H_2SO_4 at a scan rate of 50 mV s^{-1}. The CA curves were obtained by polarizing at 0.18 V for 600 s in the above-mentioned solution. The CP measurements were carried out with an anodic current of 1 mA for 60 s.

All electrochemical experiments were carried out on an electrochemical workstation (CH Instrument 660A, CHI company) using a conventional three-electrode glassy cell. A platinum sheet (12 mm × 12 mm) and an $Hg|Hg_2SO_4$, K_2SO_4 electrode (0.64 V vs. normal hydrogen electrode) were respectively served as the counter and reference electrodes. Before each test, the solution was purged with N_2 for 15 min to eliminate the dissolved oxygen. And all electrochemical experiments were performed at room temperature.

3. Results and discussion

3.1. Morphology characterization and compositional analysis

Fig. 1 shows the TEM images of the as-prepared $PtRuMoO_x$ and $PtRuWO_x$ catalysts supported on MWCNTs. It is very clear that catalyst nanoparticles are highly and homogeneously dispersed on the surface of MWCNTs. These nanoparticles are separated from each other and do not aggregate to form larger clusters. The particle size distribution for each catalyst analyzed by Image J software (Fig. 2) showed that the as-prepared catalysts have very narrow particle size distribution. $PtRuMoO_x$ and $PtRuWO_x$ nanoparticles are in the diameter ranges of 2.2–4.4 nm and 2.2–3.9 nm with the average particle sizes of 3.14 nm and 3.06 nm, respectively. The fine particle and narrow particle size distribution could be attributed to our novel synthesis approach, i.e., ultrasonic-assisted chemical reduction. During the preparing process, ultrasonication might play a crucial role in inhibiting particle size growth and equalizing their sizes, and moreover, effectively preventing agglomeration of nano-sized particles. This novel approach could be extended to prepare similar catalysts such as PtRuFe, PtRuCo, PtRuNi, $PtRuSnO_x$.

The composition of $PtRuMoO_x$/MWCNTs (Fig. 3a) and $PtRuWO_x$/MWCNTs (Fig. 3b) were analyzed by EDX. The EDX spectra show dispersive peaks of carbon, oxygen, platinum, ruthe-

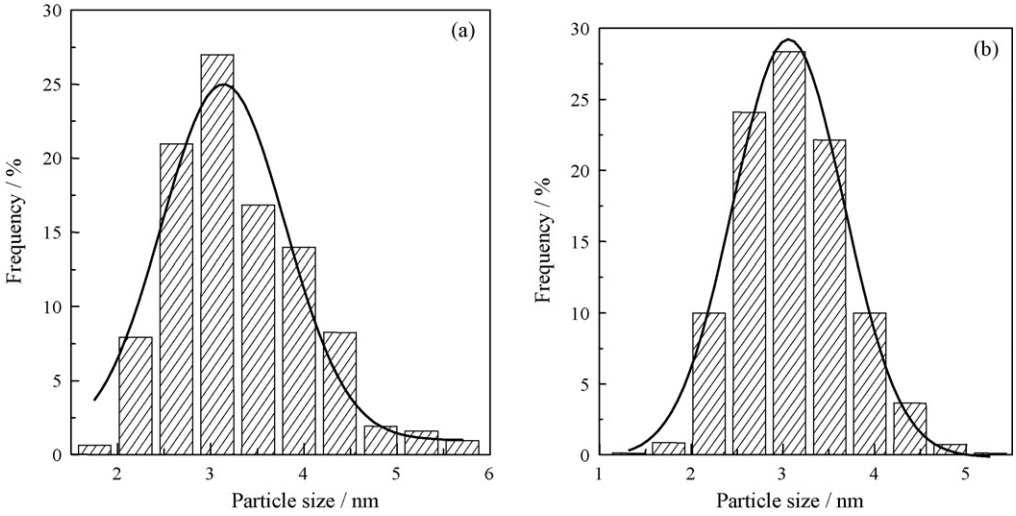

Fig. 2. Histograms of particle size distribution of (a) $PtRuMoO_x$; (b) $PtRuWO_x$.

nium, molybdenum, tungsten and copper. It is obvious that the copper peak is caused by the copper grid used to support the catalysts. The carbon comes from the MWCNTs support. EDX semiquantitative analysis indicated the atomic ratios of Pt:Ru:Mo and Pt:Ru:W are 4.6:2.7:1.0 and 5.0:1.5:1.0, respectively.

3.2. Structure characterization

Fig. 4 shows the typical XRD patterns of the as-prepared MWCNTs-supported catalysts. All the XRD patterns clearly display the characteristic peaks of MWCNTs support at $2\theta = 25.9^\circ$. The peaks at around 39.7°, 46.2°, 67.5°, 81.5° in Fig. 4a can be attributed to the diffraction of crystal faces Pt (1 1 1), Pt (2 0 0), Pt (2 2 0) and Pt (3 1 1) respectively, which means Pt exists as face-centered cubic structure. For PtRu/MWCNTs (Fig. 4b), similar diffraction peaks was observed with the diffraction angles slightly shifting to higher 2θ values, suggesting that some ruthenium alloys with platinum. For $PtRuMoO_x$/MWCNTs (Fig. 4c) and $PtRuWO_x$/MWCNTs (Fig. 4d), no additional diffraction peaks were detected, which demonstrates that MoO_x and WO_x may exist as an amorphous state. The lattice parameter (l) of platinum could be calculated from XRD patterns. The calculated lattice parameters of Pt are 3.923, 3.901, 3.908 and 3.907 Å for Pt/MWCNTs, PtRu/MWCNTs, $PtRuMoO_x$/MWCNTs and $PtRuWO_x$/MWCNTs, respectively. It can be seen that the lattice parameters for PtRu, $PtRuMoO_x$ and $PtRuWO_x$ are smaller than that of Pt, which may arise primarily from the substitution of Pt atoms by Ru atoms. An attempt was also carried out to estimate approximately the degree of PtRu alloying by the variation of lattice parameters, based on the Vegard's law [25–27]:

$$l_s = l_{Pt} - kx_{Ru} \quad (1)$$

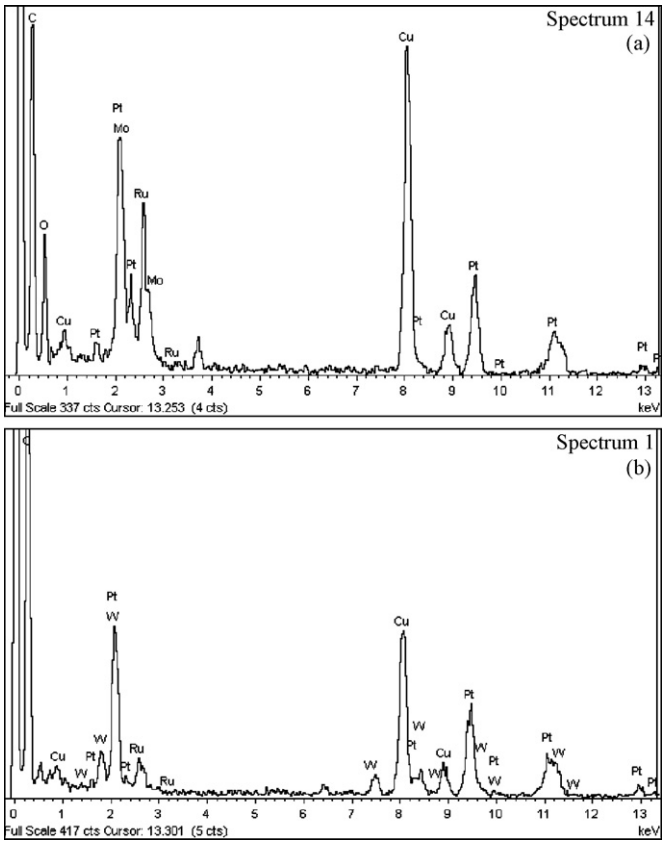

Fig. 3. EDX spectra of (a) $PtRuMoO_x$/MWCNTs; (b) $PtRuWO_x$/MWCNTs.

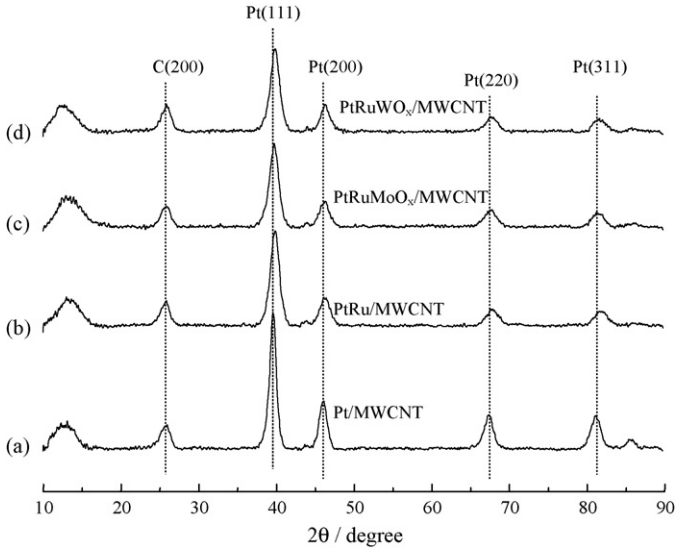

Fig. 4. XRD patterns of (a) Pt/MWCNTs; (b) PtRu/MWCNTs; (c) $PtRuMoO_x$/MWCNTs; (d) $PtRuWO_x$/MWCNTs.

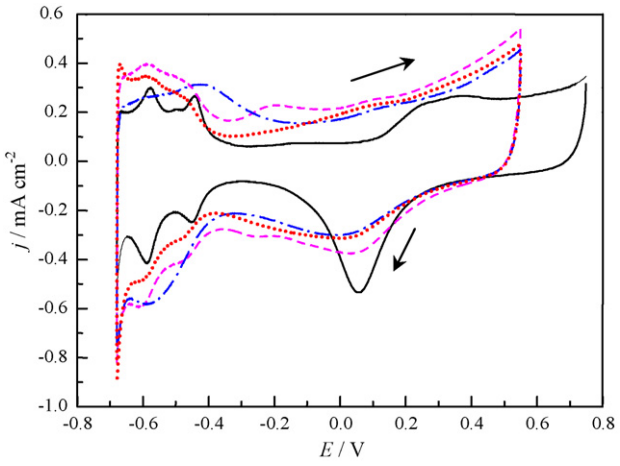

Fig. 5. Cyclic voltammograms of the as-prepared catalysts in 0.5 M H_2SO_4 solution. (—) Pt/MWCNTs; (- - -) $PtRuMoO_x$/MWCNTs; (···) PtRu/MWCNTs; (-·-·-) $PtRuWO_x$/MWCNTs.

where l_s is the lattice parameter of each Pt-based catalyst, l_{Pt} is the lattice constant of pure platinum, calculated from XRD patterns. k is a constant, whose value is 0.124 Å; and x_{Ru} is the atomic fraction of Ru in the as-prepared Pt-based catalysts. According to the formula (1), the degrees of PtRu alloying for PtRu, $PtRuMoO_x$ and $PtRuWO_x$ can be obtained at approximately 17.7, 12.1 and 13.2%, respectively. With the addition of non-noble metal oxides to PtRu, the degree of PtRu alloying slightly decreases.

3.3. Electrochemical characterization

Fig. 5 displays the CV curves for the as-prepared catalysts in 0.5 M H_2SO_4 solution at a scan rate of 50 mV s^{-1}. Well-defined CV feature of a Pt polycrystalline electrode is observed on Pt/MWCNTs. There are two pairs of redox peaks at around −0.60 and −0.45 V, which can be ascribed to hydrogen adsorption/desorption on Pt crystal face sites. Comparing with Pt/MWCNTs, there is a noticeable change observed for PtRu/MWCNTs, which is the broader feature of the double layer charging current from −0.40 V to −0.15 V. The increase in the double layer charging current is a typical characteristic of polycrystalline ruthenium [28]. For $PtRuMoO_x$/MWCNTs, the electrical double layer charging current is broader than that of PtRu/MWCNTs. Furthermore, there is a pair of redox peaks in the potential range from −0.30 V to −0.10 V, which can be attributed to the oxidation/reduction of MoO_2/MoO_3 [18,29]. For $PtRuWO_x$/MWCNTs, there are an anodic peak at −0.40 V and a reduction peak at −0.55 V, which are related to the oxidation/reduction process of the W oxides [20]. The electrochemical active surface area (*EAS*) can be calculated from the electrical charge of hydrogen adsorption (Q_H, mC) integrated from the CV curves, assuming that monolayer hydrogen atom coverage and the hydrogen adsorption electrical charge is 0.21 mC for 1 cm^2 smooth Pt surface, according to the formula $EAS = Q_H/0.21$ [30]. The calculated *EAS* are 0.87, 0.89, 0.95 and 1.06 cm^2 for Pt/MWCNTs, PtRu/MWCNTs, $PtRuMoO_x$/MWCNTs and $PtRuWO_x$/MWCNTs, respectively. Obviously, $PtRuMoO_x$ and $PtRuWO_x$/MWCNTs have higher electrochemical active surface areas which may be related to the small particle size and narrow particle distribution of the catalysts.

3.4. Electrocatalytic properties for methanol oxidation

Fig. 6 shows cyclic voltammograms of methanol electrooxidation on the as-prepared catalysts in a solution of 0.5 M CH_3OH and 0.5 M H_2SO_4 at a scan rate of 50 mV s^{-1}. The catalytic activity was evaluated as mass specific current (MSC, shown in Fig. 6a) and surface specific current (SSC, normalized to electrochemical active surface area, shown in Fig. 6b). It can be clearly seen that the onset potential for methanol electro-oxidation on Pt, PtRu, $PtRuMoO_x$, $PtRuWO_x$ are different, i.e. the onset potentials for methanol oxidation on PtRu, $PtRuMoO_x$ and $PtRuWO_x$ are more negative than that on Pt catalyst, shifting negatively by about 0.20 V. In the forward scan, methanol oxidation produced an anodic peak and in the reverse scan, there was also an oxidation peak, which is attributed to the reduction of the oxidized Pt oxide and the removal of the incompletely oxidized carbonaceous species formed in the forward scan [31–33]. From Fig. 6a, it can be seen that both $PtRuMoO_x$/MWCNTs and $PtRuWO_x$/MWCNTs catalysts have higher MSC than PtRu/MWCNTs and Pt/MWCNTs, which means this facile synthesis route can provide lower cost of ternary catalysts for DMFC. From Fig. 6b, the catalyst of $PtRuMoO_x$/MWCNTs has highest SSC, while Pt has the lowest one. The rank of MSC for methanol electroxidation is in the order of $PtRuMoO_x$/MWCNTs ~ $PtRuWO_x$/MWCNTs > PtRu/MWCNTs > Pt/MWCNTs and the SSC is in the order of $PtRuMoO_x$/MWCNTs > $PtRuWO_x$/MWCNTs > PtRu/MWCNTs > Pt/MWCNTs. It is very obvious that well-dispersed $PtRuMoO_x$/MWCNTs and $PtRuWO_x$/MWCNTs catalysts have better electrocatalytic activities for methanol oxidation than Pt/MWCNTs and PtRu/MWCNTs in both terms of MSC and SSC.

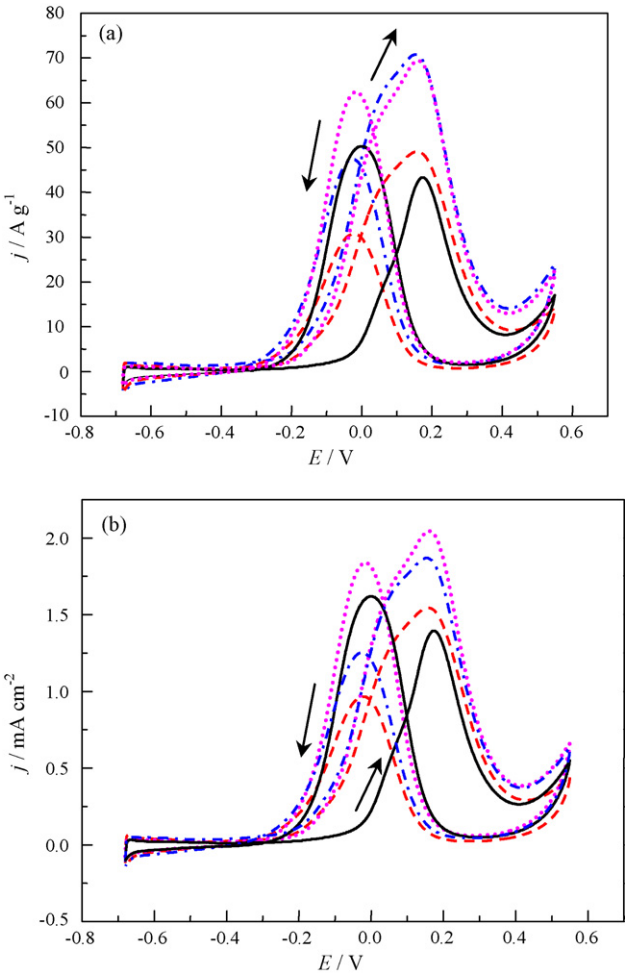

Fig. 6. Cyclic voltammograms of methanol electrooxidation on different catalysts in a solution of 0.5 M CH_3OH and 0.5 M H_2SO_4. (a) Mass specific current; (b) surface specific current. (—) Pt/MWCNTs; (- - -) PtRu/MWCNTs; (···) $PtRuMoO_x$/MWCNTs; (-·-·-) $PtRuWO_x$/MWCNTs.

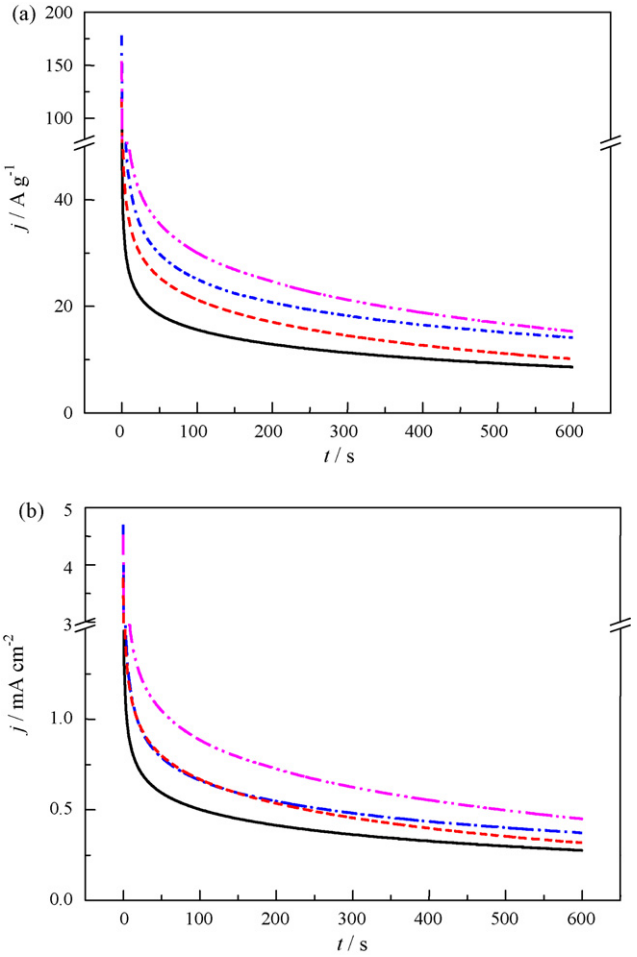

Fig. 7. Chronoamperometry measurements of methanol oxidation on different catalysts at 0.18 V in a solution of 0.5 M CH_3OH and 0.5 M H_2SO_4. (a) Mass specific current; (b) surface specific current. (—) Pt/MWCNTs; (- - -) PtRu/MWCNTs; (– ·· –) $PtRuMoO_x$/MWCNTs; (– · · · –) $PtRuWO_x$/MWCNTs.

The plots of current density (expressed by MSC and SSC) vs. time for electrochemical oxidation of methanol at 0.18 V on different catalysts with the method of chronoamperometry were compared in Fig. 7 reflecting the activity and stability of different catalysts. The methanol electrooxidation on $PtRuMoO_x$/MWCNTs possesses the highest initial and limiting current densities (including MSC and SSC), which indicates the best catalytic activity and stability for methanol oxidation, whereas Pt/MWCNTs has the lowest. Comparing with PtRu/MWCNTs, even $PtRuWO_x$/MWCNTs has similar SSC, it has higher MSC.

Fig. 8 gives the chronopotentiometry measurements of methanol oxidation with an anodic current of 1 mA on different catalysts in a solution of 0.5 M CH_3OH and 0.5 M H_2SO_4. The potential rank is in the order of $PtRuWO_x$/MWCNTs < $PtRuMoO_x$/MWCNTs < PtRu/MWCNTs, which demonstrates that $PtRuWO_x$/MWCNTs and $PtRuMoO_x$/MWCNTs have better catalytic activity. Potential oscillation with an amplitude of 0.10 V and a frequency of 0.45 Hz can be only observed for Pt/MWCNTs at this test condition. Such oscillation is often observed in the case of methanol or formic acid electrooxidation on platinum electrode where CO is formed as an intermediate [34,35].

The ternary catalysts of $PtRuMoO_x$ and $PtRuWO_x$ supported on MWCNTs have higher electrochemical catalytic activities for methanol oxidation than PtRu/MWCNTs which might be related to the highly dispersion catalysts discussed above. The enhanced performance for methanol oxidation of $PtRuMoO_x$/MWCNTs and

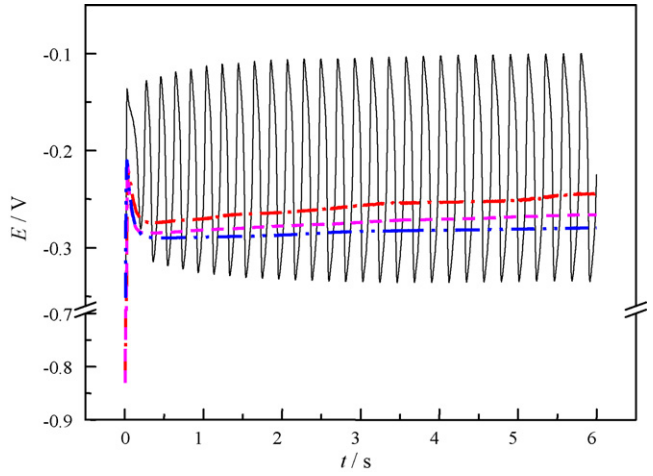

Fig. 8. Chronopotentiometry measurements of methanol oxidation with an anodic current of 1 mA on different catalysts in a solution of 0.5 M CH_3OH and 0.5 M H_2SO_4. (—) Pt/MWCNTs; (– · –) PtRu/MWCNTs; (- - -) $PtRuMoO_x$/MWCNTs; (– ·· –) $PtRuWO_x$/MWCNTs.

$PtRuWO_x$/MWCNTs can be ascribed to the addition of metal oxides (MoO_x or WO_x) to PtRu. The role of additional oxides combined with PtRu could be explained by a bifunctional mechanism, hydrogen-spillover phenomena and modification of Pt electronic states [36]. The third metal oxide could promote water activation, which generates more species of $-OH_{ads}$ to oxidize CO-like intermediates and release more active reaction sites of Pt. Compared with $PtRuWO_x$/MWCNTs, the better electrochemical performance of $PtRuMoO_x$/MWCNTs, might be due to the fact that mixed MoO_x oxides with distinct Magneli phase are relatively stable in acid media and have relatively high electronic conductivities [37].

4. Conclusions

Well-dispersed $PtRuMoO_x$ and $PtRuWO_x$ nanoparticles supported on MWCNTs were successfully synthesized by ultrasonic-assisted chemical reduction method. The average particle sizes are of 3.14 nm and 3.06 nm for $PtRuMoO_x$ and $PtRuWO_x$ with a very narrow particle size distribution in the diameter ranges of 2.2–4.4 nm and 2.2–3.9 nm, respectively. Platinum in each catalyst has face-centered cubic structure. Ru is alloyed with platinum and non-noble metal oxides exist as an amorphous state. Electrochemical measurements showed that $PtRuMoO_x$ and $PtRuWO_x$ have enhanced electrocatalytic activities for methanol oxidation than Pt and PtRu. The addition of the third metal oxide (MoO_x or WO_x) to PtRu not only increases the electrochemical active surface area, but also generates more species of $-OH_{ads}$ to oxidize CO-like intermediates and release more active reaction sites of Pt, which account for the improved stability. This novel approach could be extended to prepare similar catalysts such as PtRuFe, PtRuCo, PtRuNi, $PtRuSnO_x$ with small and even particle sizes.

Acknowledgements

This work is financially supported by a grant from the Key Program of Basic Research of the Shanghai Committee of Science and Technology (Grant No. 08JC1402000) and Science & Technology Commission of Shanghai Municipality (08DZ2270500), China.

References

[1] C.K. Dyer, J. Power Sources 106 (2002) 31–34.
[2] M.A. Hickner, B.S. Pivovar, Fuel Cells 5 (2005) 213–229.
[3] M. Winter, R.J. Brodd, Chem. Rev. 104 (2004) 4245–4270.

[4] N. Markovic, H.A. Gasteiger, P.N. Ross, X.D. Jiang, I. Villegas, M.J. Weaver, Electrochim. Acta 40 (1995) 91–98.
[5] V.S. Bagotzky, Y.B. Vassilye, Electrochim. Acta 12 (1967) 1323–1343.
[6] S. Gilman, J. Phys. Chem. 68 (1964) 70–80.
[7] C. Roth, N. Benker, R. Theissmann, R.J. Nichols, D.J. Schiffrin, Langmuir 24 (2008) 2191–2199.
[8] S. Papadimitriou, A. Tegou, E. Pavlidou, G. Kokkinidis, S. Sotiropoulos, Electrochim. Acta 52 (2007) 6254–6260.
[9] C. Roychowdhury, F. Matsumoto, V.B. Zeldovich, S.C. Warren, P.F. Mutolo, M. Ballesteros, U. Wiesner, H.D. Abruna, F.J. DiSalvo, Chem. Mater. 18 (2006) 3365–3372.
[10] O.A. Petrii, J. Solid State Electrochem. 12 (2008) 609–642.
[11] J. Zhu, F.Y. Cheng, Z.L. Tao, J. Chen, J. Phys. Chem. C 112 (2008) 6337–6345.
[12] L.X. Yang, R.G. Allen, K. Scott, P. Christenson, S. Roy, J. Power Sources 137 (2004) 257–263.
[13] M. Götz, H. Wendt, Electrochim. Acta 43 (1998) 3637–3644.
[14] A. Oliveira Neto, E.G. Franco, E. Arico, M. Linardi, E.R. Gonzalez, J. Eur. Ceram. Soc. 23 (2003) 2987–2992.
[15] A. Lima, C. Coutanceau, J.M. Leger, C. Lamy, J. Appl. Electrochem. 31 (2001) 379–386.
[16] Z. Jusys, T.J. Schmidt, L. Dubau, K. Lasch, L. Jorissen, J. Garche, R.J. Behm, J. Power Sources 105 (2002) 297–304.
[17] K. Lasch, L. Jorissen, J. Garche, J. Power Sources 84 (1999) 225–230.
[18] C. Roth, M. Goetz, H. Fuess, J. Appl. Electrochem. 31 (2001) 793–798.
[19] L.D. Burke, O.J. Murphy, J. Electroanal. Chem. 101 (1979) 351–361.
[20] M.B. de Oliveira, L.P.R. Profeti, P. Olivi, Electrochem. Commun. 7 (2005) 703–709.
[21] S.F. Zheng, J.S. Hu, L.S. Zhong, L.J. Wan, W.G. Song, J. Phys. Chem. C 111 (2007) 11174–11179.
[22] S. Ijima, Nature 354 (1991) 56–58.
[23] M. Endo, K. Takeuchi, S. Igarashi, K. Kobori, M. Shiraishi, H.W. Kroto, J. Phys. Chem. Solids 54 (1993) 1841–1848.
[24] T.J. Schmidt, H.A. Gasteiger, G.D. Stab, P.M. Urban, D.M. Kolb, R.J. Behm, J. Electrochem. Soc. 145 (1998) 2354–2358.
[25] E. Antolini, F. Cardellini, L. Giorgi, J. Mater. Sci. Lett. 19 (2000) 2099–2103.
[26] F. Sen, G. Gokagac, Energy Fuels 22 (2008) 1858–1864.
[27] D. Chu, S. Gilman, J. Electrochem. Soc. 143 (1996) 1685–1690.
[28] S.H. Yoo, S. Park, Electrochim. Acta 53 (2008) 3656–3662.
[29] K. Machida, M. Enyo, J. Electrochem. Soc. 137 (1990) 1169–1175.
[30] A.J. Bard, Electroanal. Chem., Marcel Dekker, 1976.
[31] W.L. Xu, T.H. Lu, C.P. Liu, W. Xing, J. Phys. Chem. B 109 (2005) 14325–14330.
[32] J. Zhu, Y. Su, F.J. Cheng, J. Chen, J. Power Sources 166 (2007) 331–336.
[33] R. Manoharan, J.B. Goodenough, J. Mater. Chem. 2 (1992) 875–887.
[34] M. Krausa, W. Vielstich, J. Electroanal. Chem. 399 (1995) 7–12.
[35] J. Lee, C. Eickes, M. Eiswirth, G. Ertl, Electrochim. Acta 47 (2002) 2297–2301.
[36] Z.B. Wang, G.P. Yin, Y.G. Lin, J. Power Sources 170 (2007) 242–250.
[37] T. Ioroi, N. Fujiwara, Z. Siroma, K. Yasuda, Y. Miyazaki, Electrochem. Commun. 4 (2002) 442–446.